Physico-chemical investigation of catalytic oxidation sites in 4%Rh/CeO2 catalysts prepared by impregnation and deposition–precipitation methods

Madona Labaki, Samer Aouad, Sara Hany, Cynthia Abou Serhal, Edmond Abi-Aad, Antoine Aboukaïs

Version of Record: https://www.sciencedirect.com/science/article/pii/S030101041930624X
Manuscript_90b2d3b56d1cb347b07b3a9806dfc9e6

Physico-chemical investigation of catalytic oxidation sites in 4%Rh/CeO_2 catalysts prepared by impregnation and deposition–precipitation methods

Madona Labaki [a,b], Samer Aouad [a,c], Sara Hany [a], Cynthia Abou Serhal [a,b], Edmond Abi-Aad [a], Antoine Aboukaïs [a*]

[a] *Unité de Chimie Environnementale et Interactions sur le Vivant EA 4492 (UCEIV), MREI, Université du Littoral – Côte d'Opale (ULCO), 145 avenue Maurice Schumann, 59140 Dunkerque, France*

[b] *Laboratory of Physical Chemistry of Materials (LPCM/PR2N), Faculty of Sciences, Lebanese University, Fanar, 90656 Jdeidet El Metn, Lebanon*

[c] *Department of Chemistry, Faculty of Sciences, University of Balamand, P.O. Box. 100, Tripoli, Lebanon*

*Corresponding author

E-mail address: aboukais@univ-littoral.fr

Tel : +33.3.28.65.82.68 Fax : +33.3.28.65.82.39

E-mail addresses:

Madona Labaki: mlabaki@ul.edu.lb; **Samer Aouad:** samer.aouad@balamand.edu.lb; **Sara Hany:** sarahani@hotmail.com; **Cynthia Abou Serhal:** cynthia.abou-serhal@univ-littoral.fr; **Edmond Abi-Aad:** edmond.abiaad@univ-littoral.fr; **Antoine Aboukaïs:** aboukais@univ-littoral.fr

Abstract

4 wt % Rh/CeO_2 catalysts were prepared by two different methods: deposition-precipitation (DP) and impregnation (Imp). X-ray diffraction (XRD), differential scanning calorimetry and thermogravimetry (DSC-TG), temperature-programmed reduction (TPR), and electron paramagnetic resonance (EPR) were used for physicochemical characterization. The solids were tested in propylene and carbon black oxidation reactions. The 4%Rh/CeO_2 (DP) showed better catalytic performance in both reactions compared to the catalyst prepared by the impregnation method. The XRD technique evidenced the formation of Rh_2O_3 phase in the DP-

solid after calcination of this latter at 400 °C for 4 h. EPR evidenced, only in the DP-solid, the presence of O_2^- species in interaction with the CeO_2 surface whereas Rh^{4+} ions in the form of clusters were identified in both solids. The TPR technique showed that the DP-solid was reduced by hydrogen at lower temperature compared to the impregnated one. The higher catalytic performance of the DP-solid was attributed to the presence of O_2^- species along with the presence of Rh_2O_3 phase in ceria and to the better reducibility and lower particle size of the rhodium species.

Keywords: *CeO_2 ; deposition-precipitation ; impregnation ; O_2^- species ; oxidation ; Rh ; Rh_2O_3.*

I. Introduction

Ceria (CeO_2) has a great reputation in catalysis and was well investigated due to its high oxygen storage capacity and its use in catalytic oxidation reactions [1-3]. It is also well known that adding transition metals over ceria enhances the activity of the latter [4-5].

Rhodium supported on CeO_2 is extensively used as catalyst in many reforming reactions and it is also involved in a number of oxidation reactions [6-12]. Haneda et al. [6] have shown that the Ir-Rh/CeO_2-ZrO_2 improves three-way catalytic activity by oxidizing CO and C_3H_6 molecules and reducing NO one. Shimizu et al. [7] have prepared Rh/CeO_2 catalysts by a supercritical CO_2 impregnation technique and they used them for automotive exhaust. The catalysts have been characterized by energy-dispersive X-ray spectroscopy (EDX), X-ray diffraction (XRD), and transmission electron microscopy (TEM) to analyze the Rh loading, Rh structure, and the morphology of the particles, respectively. Li et al. [8] have investigated Rh/CeO_2-SiC catalyst in the partial oxidation of ethanol for hydrogen production. Cuauhtémoc et al. [9] have used Rh/γ-Al_2O_3-CeO_2 as catalyst to oxidize gasoline oxygenates by wet air.

The EPR technique is highly sensitive compared to other spectroscopic techniques (XPS, IR, UV–visible, etc.) making it suitable for the investigation of adsorbed paramagnetic species at

solid surfaces. These paramagnetic species can be intermediate compounds implied in catalytic oxidation and reduction reactions. Therefore, their identification could help in accessing reactions mechanisms which depend on the redox properties of the active sites located at the support surface and the support itself.

The aim of the present study is to compare the catalytic performances of two series of 4%Rh/CeO_2 catalysts (prepared by deposition-precipitation and conventional impregnation) towards the total oxidation of propylene and carbon black particles and to use physico-chemical techniques such as EPR and TPR to explain the performances obtained. Propylene is an example of the pollutants volatile organic compounds and carbon black is used as soot model.

2. Experimental part

2.1. Catalysts preparation

Cerium hydroxide was prepared by precipitation of cerium (III) nitrate hexahydrate, $Ce(NO_3)_3.6H_2O$ (ACROS) with sodium hydroxide NaOH (ACROS). The suspension was filtered, washed several times with hot deionized water, and dried at 100 °C for 24 hours. Ceria, CeO_2, was obtained by calcination under air at 400 °C for 4 hours.

The rhodium chloride $RhCl_3.xH_2O$ (STREM CHEMICALS) was used as rhodium precursor and introduced into ceria according to two methods: wet impregnation and deposition-precipitation.

Wet impregnation: The supported rhodium/CeO_2 catalysts were prepared by the conventional wet impregnation method. Ceria was impregnated with rhodium solution. The slurry was stirred 2 hours at ambient temperature and then water was slowly evaporated at 75 °C in a rotary evaporator. The as-dried sample was put in an oven set at 100 °C for 20 to 24 h. The obtained powder was calcined at 400 °C (1 °C.min^{-1}, 4 h, 2 L dried air.h^{-1}). Two rhodium

loadings were prepared: 0.5 wt % and 4 wt %. The samples will be respectively designated by 0.5% Rh/CeO_2 (Imp) and 4% Rh/CeO_2 (Imp).

Deposition-precipitation: Rhodium (4 wt %) was loaded on ceria preliminary suspended in water. The precipitation was carried under control of the following parameters: pH was maintained constant at 8 by adding drops of 0.1 mol.L^{-1} NaOH solution, the temperature was fixed at 80 °C, and the stirring speed was constant. The slurry was stirred during four hours, filtered, washed with hot water, dried overnight in an oven 100 °C, and then calcined at 400 °C (1 °C.min^{-1}, 4 h, 2 L dried air.h^{-1}). The sample will be designated by 4% Rh/CeO_2 (DP).

2.2. Catalysts characterization

The X-ray diffraction (XRD) measurements were performed with an automatic powder diffractometer BRÜKER AXS D8 Advance, using CuKα radiation and a scintillation counter LynxEye. The diffraction patterns were recorded in a step-scan mode with a step of 0.02 ° (2 θ), counting time 2 s, in the angular interval 20-80 ° at room temperature. The Eva program was used for diffraction data processing. Identification of the crystalline phases was made with the Joint Committee on Powder Diffraction Standards (JCPDS) files from the International Center for Diffraction Data (ICDD). Differential scanning calorimetry and gravimetric analysis (DSC-TG) was conducted in air flow (75 mL.min^{-1}) at a heating rate of 5 °C.min^{-1} from room temperature to 400 °C followed by an isotherm at the same temperature for four hours with about 30 mg of sample with a Netzsch STA 409 apparatus.

The electron paramagnetic resonance (EPR) measurements were performed at two different temperatures: -196 °C and room temperature, on an EMX BRUKER spectrometer with a cavity operating at a frequency of 9.5 GHz (X band). The measurements were performed on 50 to 55 mg of the calcined solids previously treated under vacuum (1.2 x 10^{-5} bar). The

magnetic field was modulated at 100 kHz and the power supply was sufficiently low to avoid saturation effects. The *g* values were determined from precise frequency and magnetic field values.

The temperature-programmed reduction (TPR) measurements were performed on a device AMI-200 from ZETON ALTAMIRA. A trap for removing water during reduction was mounted in the gas line prior to the thermal conductivity detector. A hydrogen-argon mixture (5 % H_2/Ar) was used to reduce the samples at a flow rate of 30 mL.min^{-1}. The temperature was linearly raised at a rate of 5 ºC.min^{-1} from room temperature till 900 ºC and then the sample was kept one hour at 900 ºC. The current of the thermal conductivity detector was 75 mA. Before the reducing step, the sample was flushed by an argon flow of 30 mL.min^{-1} during one hour at 150 ºC.min^{-1} (5 ºC.min^{-1}). The sample mass used was about 50 mg.

2.3. Catalytic test

The catalysts were tested in the total oxidation of propylene. The experiments were carried out in a conventional fixed bed micro reactor between 25 °C and 500 °C (1 °C.min^{-1}). The reactive flow (100 mL.min^{-1}) consisted of a mixture of air and 6000 ppm of propylene. Before the catalytic test, the solid (100 mg) was activated under a flow of air (2 L.h^{-1}) at 400 °C (1 °C.min^{-1}). The reactants and products were identified and quantified by a Varian CP-4900 micro gas chromatography equipped with thermal conductivity detectors (TCD).

The carbon black (CB)–catalyst mixture was prepared in tight contact conditions. 2 wt % of CB and 98 wt % of catalyst were manually grinded for 15 min. About 30 mg of CB–catalyst mixture were loaded in an alumina crucible and heated from room temperature to 1000 °C (heating rate: 5 °C min^{-1}) in air flow (75 mL min^{-1}). Three characteristic temperature values are determined from differential scanning calorimetry and thermogravimetric (DSC–TG) curves (Fig. 1): T_i where the CB oxidation begins, T_{max} where the rate of oxidation is at its

maximum, and T_f where the combustion ends. T_{max} values were used to compare the catalytic performances and CB oxidation rates.

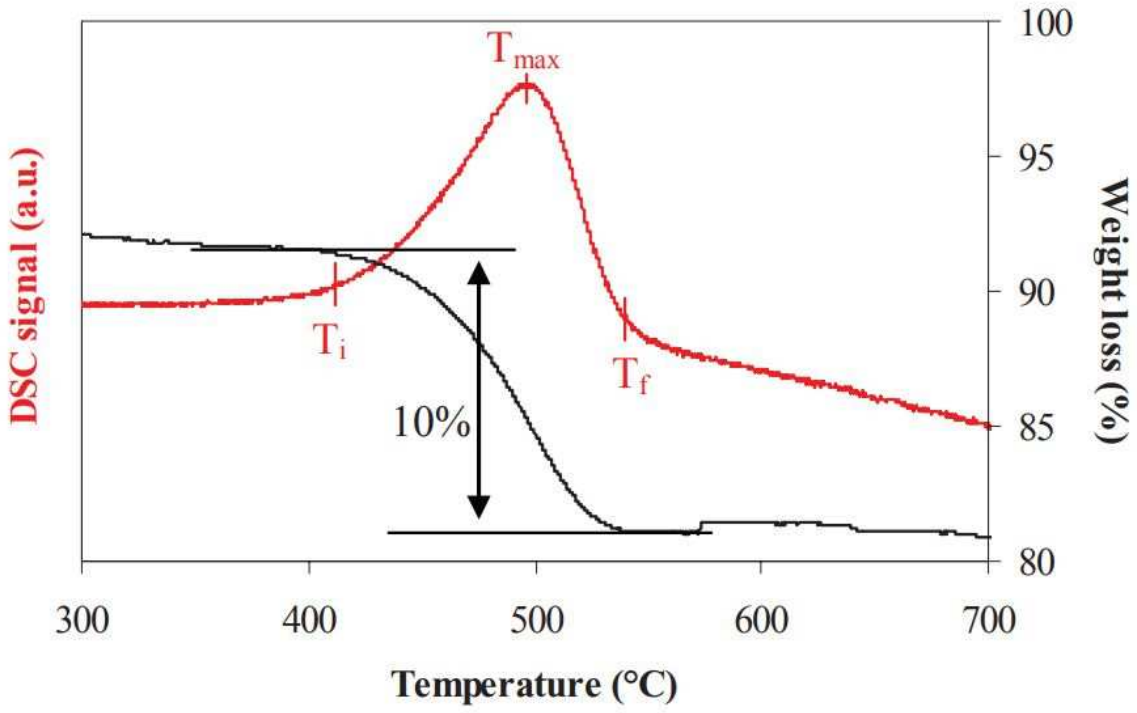

Figure 1: Determination of T_i (beginning of carbon black (CB) combustion under air), T_{max} (maximum combustion rate), and T_f (end of CB combustion) on the DSC and TG curves.

3. Results and discussion

3.1. Physico-chemical characterization

3.1.1. X-ray diffraction (XRD)

Fig. 2 shows the XRD patterns obtained for both 4% Rh/CeO_2 (DP) and (Imp). The lines attributed to CeO_2 cerianite phase (JCPDS-ICDD 34-0394) located at 2θ: 28.55 °; 33.07 °; 47.48 °; 56.34 °; 59.44 °; 69.86 °; 77.08 °; and 79.83 °, were observed for both solids. In addition, a line with a weak intensity, located at 35.2 °, was observed and assigned to Rh_2O_3 hexagonal phase (JCPDS-ICDD 41-0541). This line was absent in the XRD pattern of

4% Rh/CeO_2 (Imp). Mulukutla et al. [13] were also able to detect Rh_2O_3 by XRD in rhodium incorporated into MCM-41.

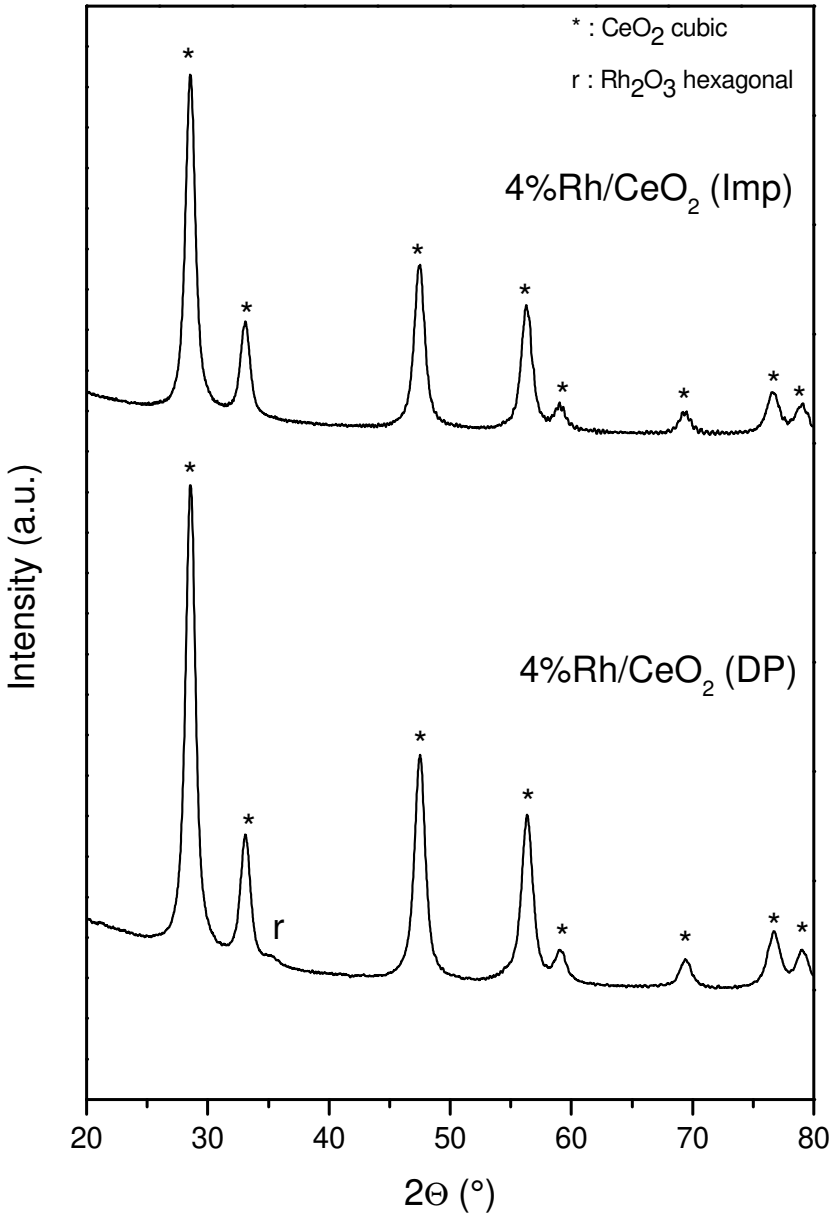

Figure 2: X-ray diffraction (XRD) patterns of: a) 4% Rh/CeO_2 (DP) and b) 4% Rh/CeO_2 (Imp).

3.1.2. Thermal analysis

Fig. 3a and Fig. 3b show the DSC and TG curves obtained respectively for 4% Rh/CeO_2 (DP) and 4% Rh/CeO_2 (Imp), before calcination, heated under dry air at a rate of 5 °C min^{-1} from room temperature up to 400 °C followed by a 4 h dwell at the final temperature.

For the DP solid, the percentage of weight loss from room temperature up to 400 °C and before the 4 h-dwell at this latter temperature is of 3.1 %. This loss occurs in two steps: the first one is due to the loss of physisorbed water on the solid (2.1 %) and the second one to the desorption of water present in $RhCl_3.xH_2O$ (1 %). Indeed, when this latter precursor was brought from room temperature up to 400 °C and kept at this temperature for 4 h (Fig. 3c), the total weight loss recorded is about 24 %. Since, in the prepared catalyst, the rhodium weight corresponds to 4 % of the catalyst total weight, the water loss resulting from the precursor dehydration must be equal to about $24 \times \frac{4}{100} = 0.96\,\%$, a value close to 1 %, the value obtained for the second loss step. In addition, the very slight gain of weight (0.1-0.2 %) after 150 min of calcination at 400 °C can be due to the oxidation of $RhCl_3$ into Rh_2O_3 -detected by XRD- and to the formation of CeOCl or Ce-Cl species on ceria surface as reported by Force et al. [10]. These formations are illustrated by the following reaction:

$$2\ RhCl_3/CeO_2 + 4\ CeO_2 + \frac{3}{2}\ O_2 \rightarrow Rh_2O_3/6ClCeO_2$$

For the Imp solid, the weight loss also takes place in two steps, with a total percentage of 4.7 %. The first step, 3.4 %, corresponds to the loss of physisorbed water and the second step, 1.3 %, to dehydration of the precursor $RhCl_3.xH_2O$. No trace of gain was detected during the 4 h-dwell at 400 °C. This result can explain the absence of Rh_2O_3 formation in the impregnated solid.

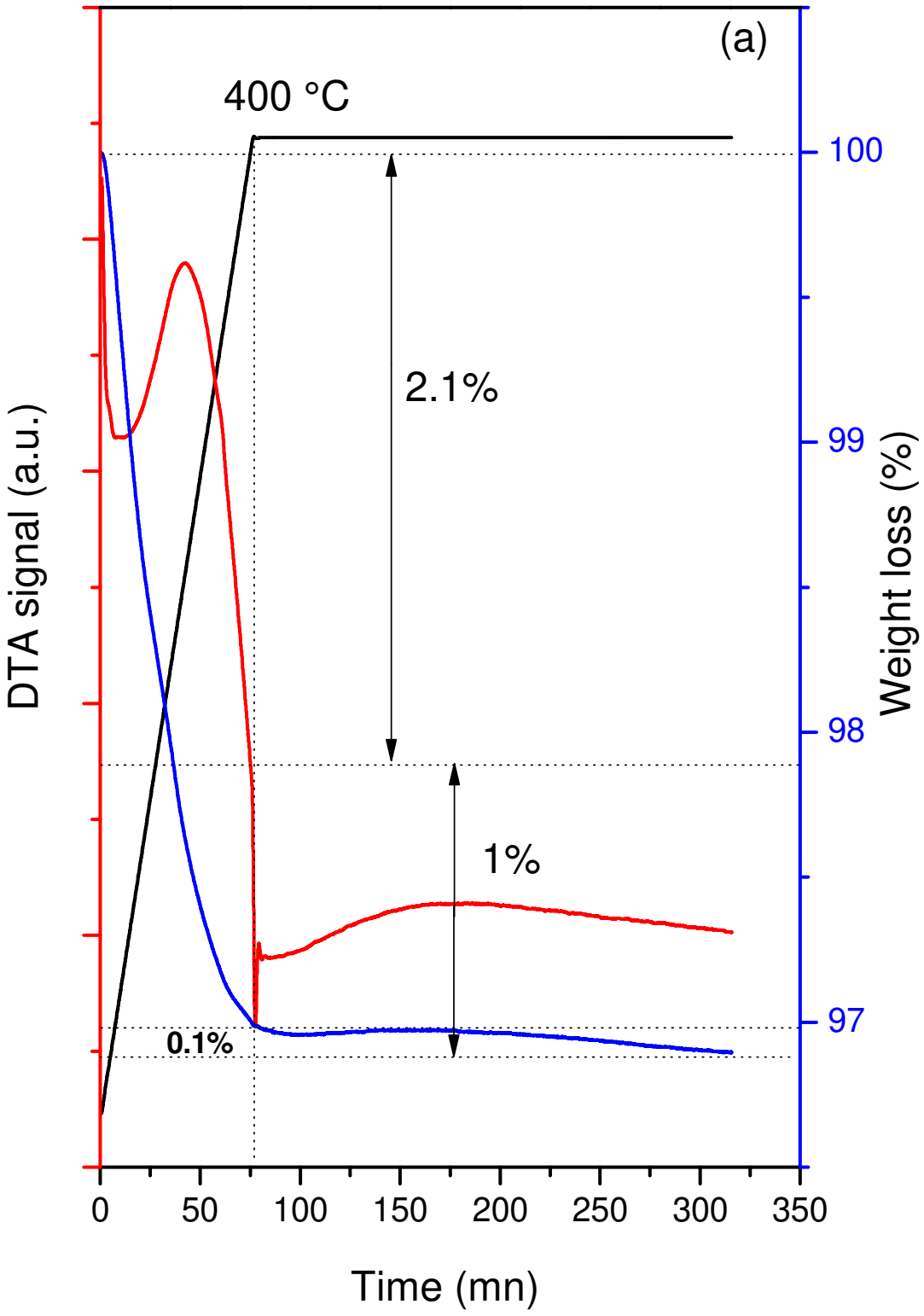
(a)
400 °C
2.1%
1%
0.1%
DTA signal (a.u.)
Weight loss (%)
100
99
98
97
0
50
100
150
200
250
300
350
Time (mn)

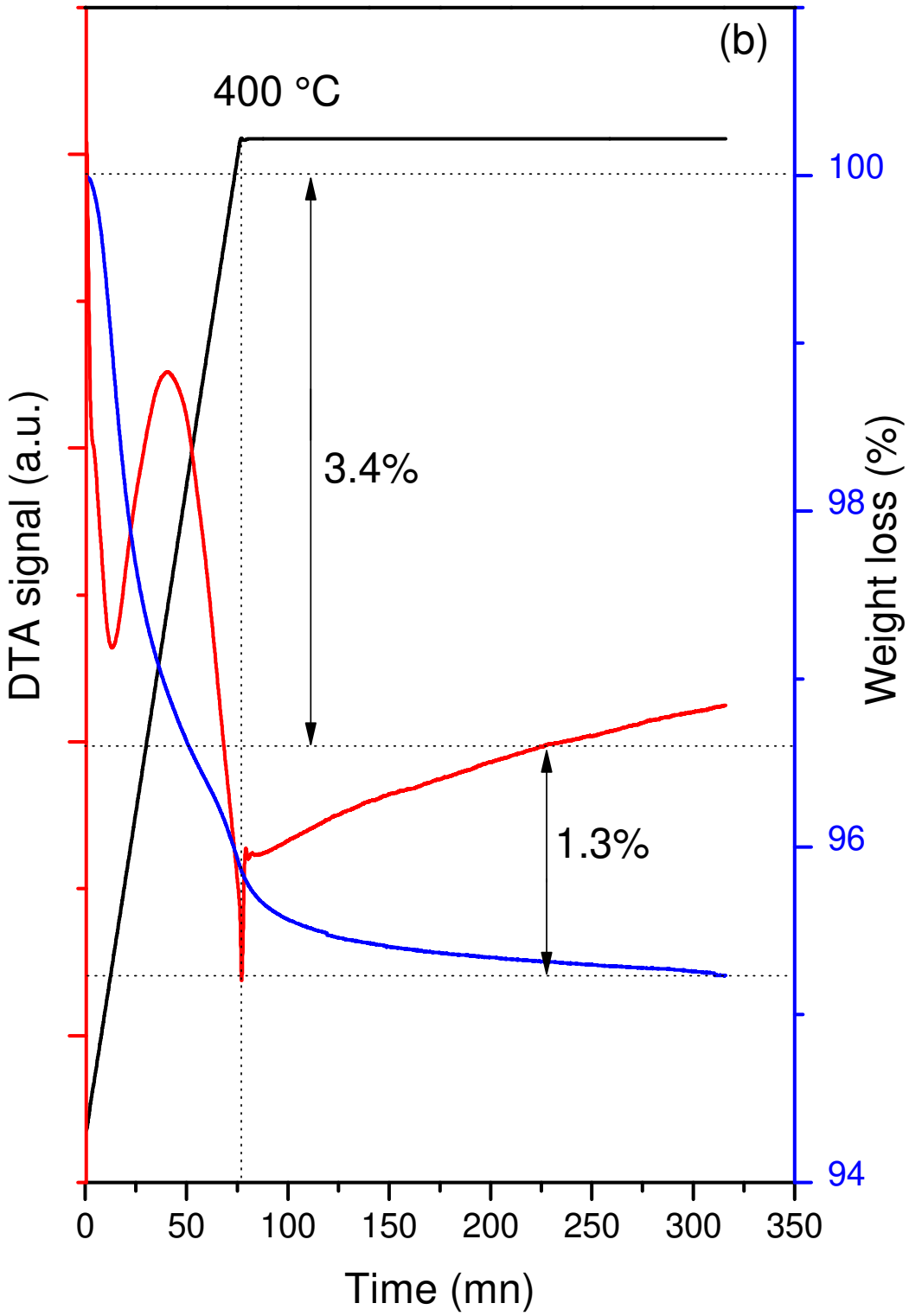
(b)
400 °C
3.4%
1.3%
DTA signal (a.u.)
Weight loss (%)
100
98
96
94
0
50
100
150
200
250
300
350
Time (mn)

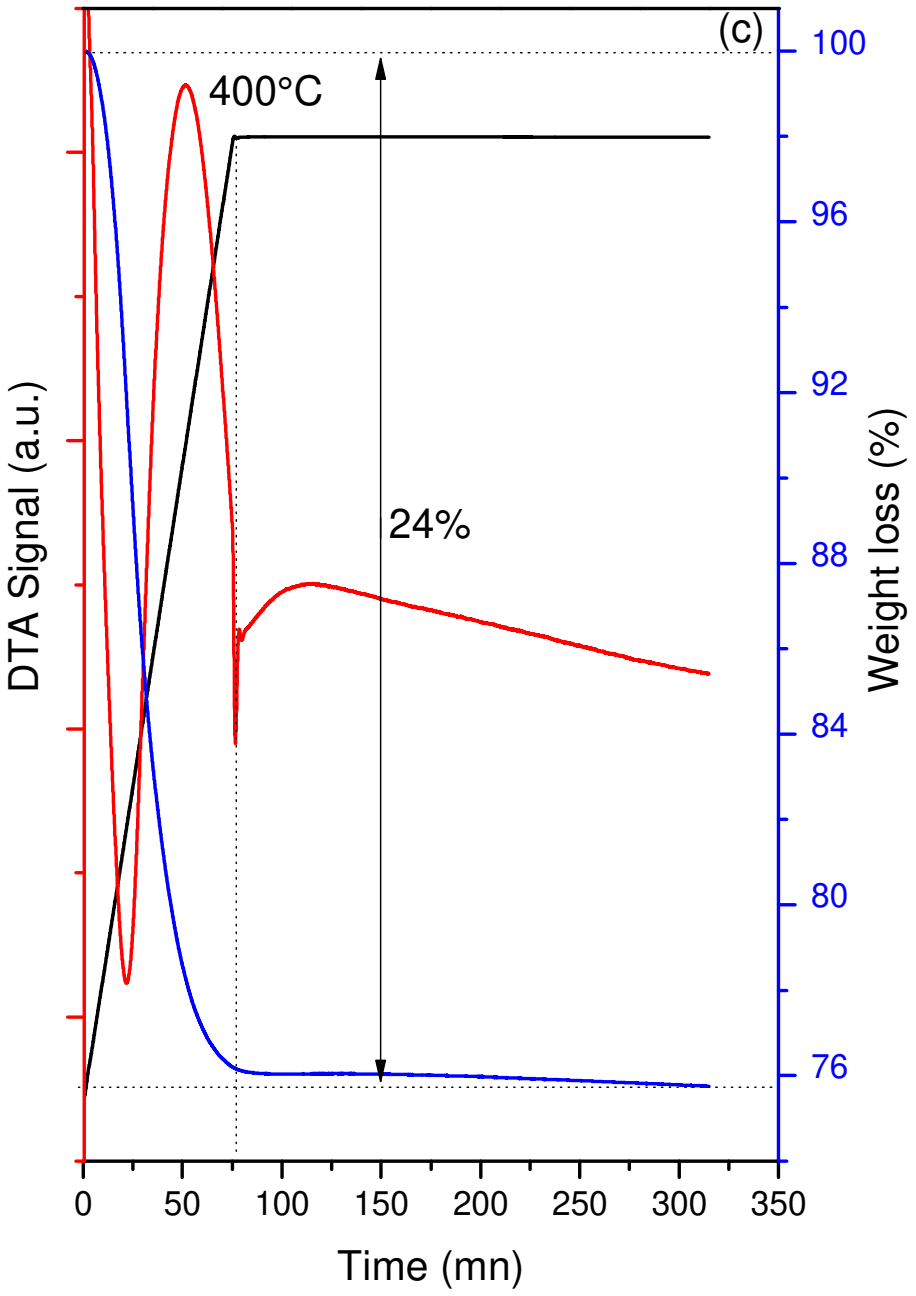

Figure 3: Differential scanning calorimetry and thermal gravimetry (DSC-TG) analysis under air flow (75 mL.min^{-1}) at a heating rate of 5 °C.min^{-1} from room temperature to 400 °C

followed by an isotherm at 400 °C for four hours: a) 4% Rh/CeO_2 (DP), b) 4% Rh/CeO_2 (Imp), and c) $RhCl_3.xH_2O$.

3.1.3. Electron paramagnetic resonance (EPR)

4% Rh/CeO_2 (DP)

The EPR spectrum, recorded at -196 °C, of 4% Rh/CeO_2 (DP) subjected to vacuum at room temperature during 1 h, is given in Fig. 4a. It is a complex spectrum. It is apparently formed by the superimposition of three signals (Fig. 4a). The first one, Ce^{3+}, has an axial symmetry with $g_\perp = 1.967$ and $g_{//} = 1.947$. This signal was extensively studied by numerous authors [3, 10, 14-15] and was attributed to Ce^{3+} ions. The second one, nominated O_D, possessing an axial symmetry with $g_{//} = 2.030$, $g_\perp = 2.010$, and $g_{iso} = 2.017$ was unambiguously attributed to O_2^- species located on Ce^{4+} ions of ceria. Indeed, a similar signal with a slight difference in the $g_{//}$ value was obtained after adsorption of molecular O_2 on pure ceria [16-19]. The O_D signal disappeared when the spectrum is recorded at room temperature (Fig. 5a). This means that the O_2^- species is weakly adsorbed on ceria. The third signal, R_D, is symmetric and centred at g = 2.17 with peak-to-peak width ΔH = 96 G. This latter can be attributed to Rh^{4+} (Z = 45; $4d^5$ with S = 5/2; 3/2; 1/2) of RhO_2 small particles [20-22]. This latter oxide can be formed beside of the Rh_2O_3 one but in an amount not detectable by XRD. In addition, since the fine structure is not observed, it could be said that S = 1/2.

The EPR spectrum, recorded at -196 °C, of 4% Rh/CeO_2 (DP) subjected to vacuum at 400 °C during 1 h, is illustrated in Fig. 4b. This kind of treatment can be considered as a smooth reduction of the solid. Apparently, beside the Ce^{3+} and R_D signals, the spectrum is formed of four signals: i) the first one O_P, apparently similar to O_D, with a little difference in the $g_{//}$

value (2.032), but, on the contrary, the O_2^- species corresponding to O_P remained stable when the spectrum is recorded at room temperature (Fig. 5b); ii) an isotropic signal, called S_D, centred at g = 2.0015 with a peak-to-peak width ΔH = 10 G, it was attributed to a trapped electron in the ceria matrix [23-24]; iii) a signal, nominated R_P, with an axial symmetry is characterized by $g_{//} = 2.16$, $A_{//} = 115$ G, $g_\perp = 1.984$, $A_\perp = 19$ G, and $g_{iso} = 2.043$ [25-28]. Since the signal possesses a hyperfine structure of two lines, it was unambiguously attributed to Rh species (I = 1/2). It is well known that the metallic rhodium (Rh^0; Z = 45; $5s^1$ $4d^8$) cannot be detected by EPR except at low temperatures (less than -196 °C) [22, 26, 29] due to the presence of the unpaired electron in the s orbital. In addition, Rh^+ ($4d^8$) and Rh^{3+} ($4d^6$ with high spin) possess respectively a total electron spin S = 1 and 2. Since the fine structure is absent in the spectrum, therefore R_P signal could not be due to such species. Rh^{3+} ($4d^6$ with low spin) has a S = 0 and is silent in EPR. Finally, the Rh^{2+} ions ($4d^7$) has S = 3/2 in high spin and S = 1/2 in low spin. Since the fine structure is absent in the spectrum, hence R_P signal could be ascribed to Rh^{2+} low spin; iv) a symmetric signal, S_P, with ΔH = 15 G and centred at g = 2.043. This latter value is equal to g_{iso} of the R_P signal, consequently it can be attributed to Rh^{2+} species in the form of clusters. Since the R_D signal, attributed to Rh^{4+} ions, remained stable after this smooth reduction, this means that the Rh^{2+} species responsible for the R_P signal can be obtained by reduction the Rh^{3+} ions of Rh_2O_3 oxide and not by the reduction of Rh^{4+} ions.

The formation of O_D and S_D signals is due to the presence of Cl^- ions, coming from the $RhCl_3$ precursor, in ceria [23, 30]. Indeed, 1 wt % Cl was impregnated on CeO_2 already calcined at 400 °C using a solution of HCl. The obtained product was calcined at 400 °C for 4 h. The EPR spectrum of this sample, after being subjected to O_2 adsorption, exhibited two signals similar to O_D and S_D (Fig. 4c). The small difference in the g values is due to the absence of rhodium on the latter solid.

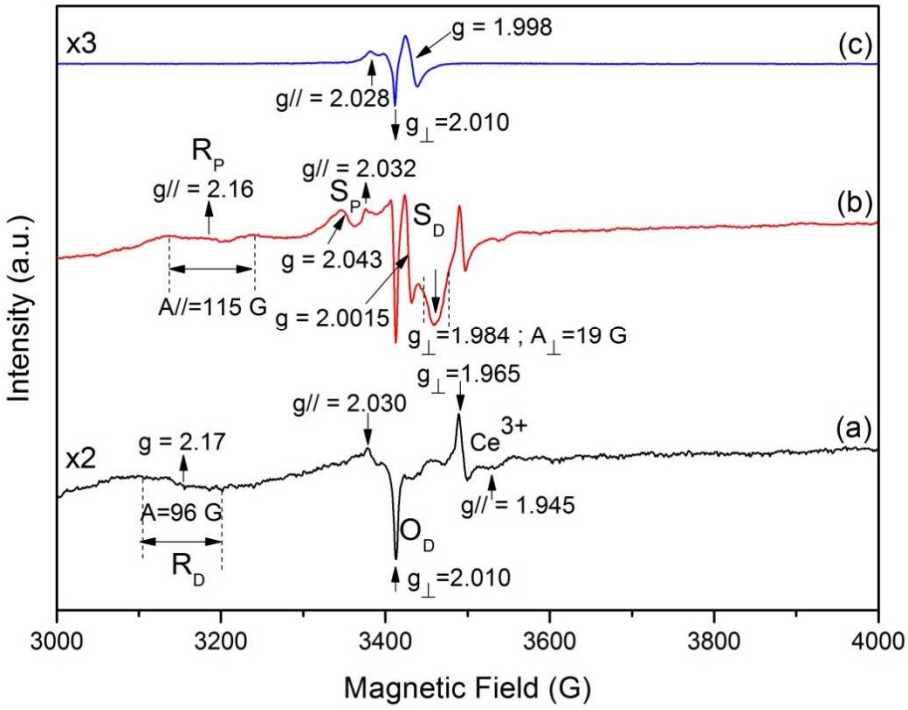

Figure 4: Electron paramagnetic resonance (EPR) spectra recorded at -196 °C of: a) 4% Rh/CeO_2 (DP) evacuated at room temperature for 1 h, b) 4% Rh/CeO_2 (DP) evacuated at 400 °C for 1 h, c) 1% HCl/CeO_2 evacuated at 400 °C for 1 h.

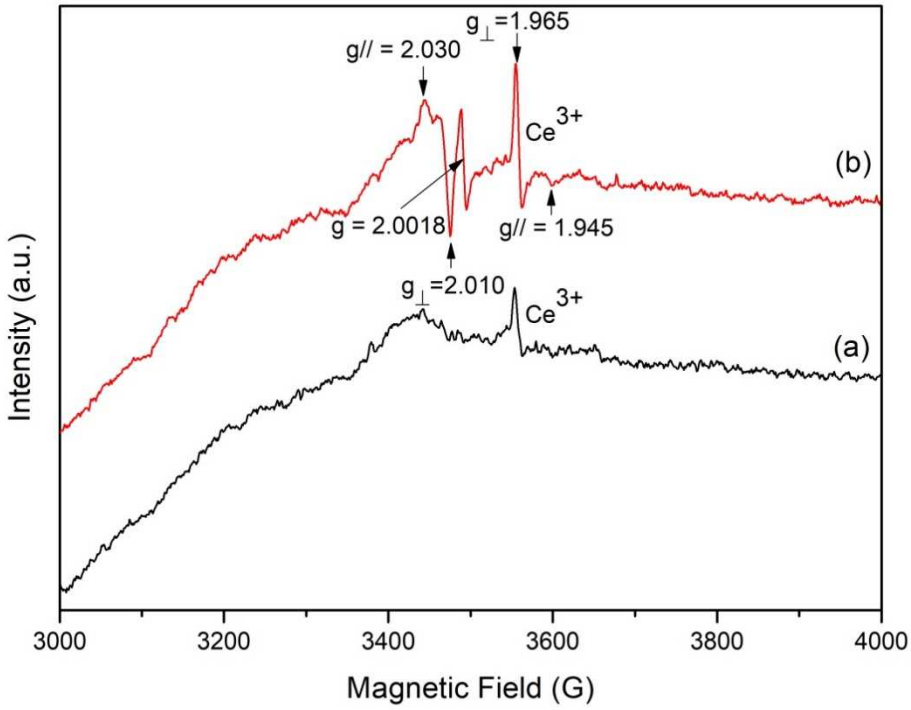

Figure 5: Electron paramagnetic resonance (EPR) spectra recorded at room temperature of: a) 4% Rh/CeO_2 (DP) evacuated at room temperature for 1 h, b) 4% Rh/CeO_2 (DP) evacuated at 400 °C for 1 h.

When the EPR spectrum of 4% Rh/CeO_2 (DP) subjected to vacuum at 400 °C during 1 h is recorded at room temperature (Fig. 5b), the R_D, R_P, and S_P disappeared whereas, the Ce^{3+}, O_P, and S_D remained observable but their intensities decreased, compared to those obtained at -196 °C, following the Curie law. The stability of O_2^- species responsible for the O_P signal is an indication of the solid oxidizing property.

4% Rh/CeO_2 (Imp)

Fig. 6a shows the EPR spectrum, recorded at -196 °C, of 4% Rh/CeO_2 (Imp) subjected to vacuum at room temperature during 1 h. The spectrum is composed of three signals: the first one was already attributed to Ce^{3+} ions, the second one, nominated R_I, is a broad symmetric signal centered at g = 2.16 with ΔH = 225 G, and the last one (D_I) is not well-resolved. When the spectrum is recorded at room temperature, the intensities of the above signals decreased following the Curie law. The R_I signal can be attributed to Rh^{4+} in the form of clusters. The oxidation of $RhCl_3$, which is in the form of large particles loaded on ceria surface due to the preparation method (impregnation), is responsible for the formation of Rh^{4+} clusters.

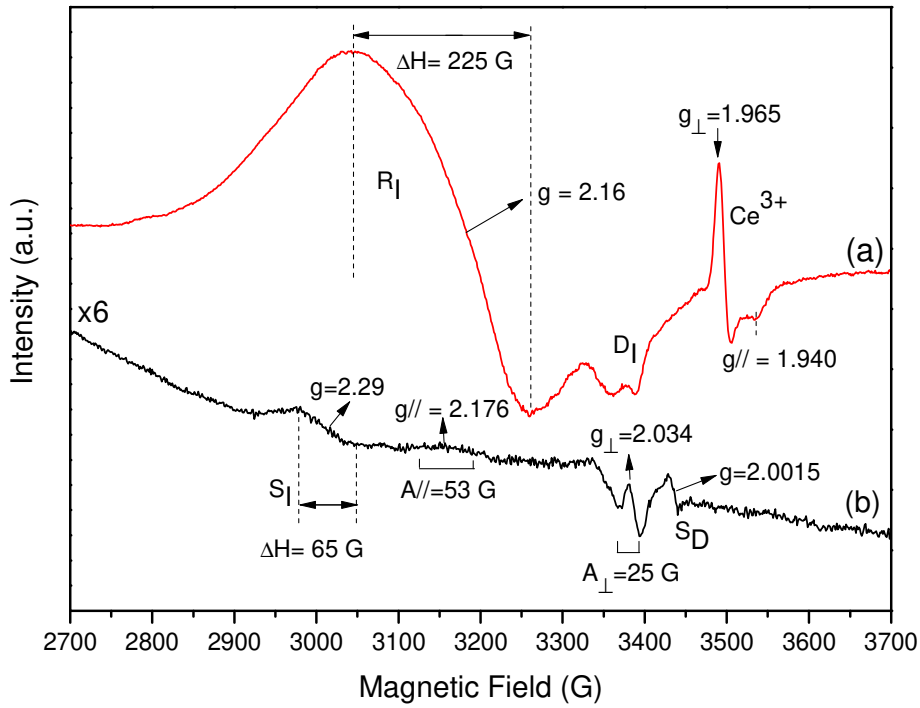

Figure 6: Electron paramagnetic resonance (EPR) spectra recorded at -196 °C of 4% Rh/CeO_2 (Imp): a) evacuated at room temperature for 1 h, b) evacuated at 400 °C for 1 h.

When the solid 4% Rh/CeO_2 (Imp) was treated under vacuum at 400 °C for 1 h (Fig. 6b), the Ce^{3+} signal and R_I one disappeared whereas the D_I signal became well resolved with an axial symmetry and a hyperfine structure of two lines ($g_{//}$ = 2.176, $A_{//}$ = 53 G, $g_{\perp}$ = 2.034, $A_{\perp}$ = 25 G, and g_{iso} = 2.081) but its intensity is very weak (Fig. 6b). Such a signal, attributed to Rh^{2+} species, was obtained in rhodium doped lithium dithionate ($Li_2S_2O_6.2H_2O$) [27]. In our sample, these species can be obtained by a soft reduction of some $RhCl_3$ species which could resist to the oxidation during the calcination because of their localisation in the bulk of large particles. The disappearance of the R_I signal can be due to the reduction of Rh^{4+} into Rh^{3+} since this latter species is in general silent toward the EPR technique. The symmetric signal with a weak intensity, centred at g = 2.0015 (S_D), can unambiguously be attributed to a trapped electron in ceria matrix. Finally, the isotropic signal S_I centred at g = 2.29 with ΔH = 65 G, can be due to traces of Rh^{2+} clusters [28, 31-32] resulting from the reduction of some Rh^{3+} species obtained after reduction of Rh^{4+} clusters.

3.1.4. Temperature-programmed reduction (TPR)

Fig. 7 shows the TPR profiles of CeO_2, 4% Rh/CeO_2 (Imp), 4% Rh/CeO_2 (DP), and 4% Rh_2O_3/CeO_2 (DP). The latter is a sample prepared by using Rh_2O_3 as precursor instead of $RhCl_3$. In the case of ceria (Fig. 7a), two broad reduction peaks were observed at 472 °C and 776 °C and were ascribed, respectively, to the reduction of ceria surface with the formation of Ce^{3+} species and an oxygen lacuna, and to the removal of bulk oxygen from the ceria structure along with the reduction of Ce^{4+} into Ce^{3+} ions [16, 33-35].

Adding rhodium to ceria, following both DP and Imp methods, leads in one side to the shift of the two reduction peaks obtained for the pure ceria to lower temperatures and in the other side to the appearance of new reduction peaks at a lower range of temperatures (< 220 °C). The

shift of ceria reduction peaks to lower temperatures suggests that rhodium makes ceria reduction easier. Furthermore, the amount of Ce^{4+} reduced into Ce^{3+} either on the surface or in the bulk of ceria, decreases after rhodium addition. The latter fact suggests a modification in ceria reduction behavior due to rhodium.

The peaks obtained at low temperatures (60 and 141 °C) for the 4% Rh/CeO_2 (DP) (Fig. 7c) can be due to Rh_2O_3 and O_2^- ions reduction. Indeed, the TPR profile of Rh_2O_3/CeO_2 (Fig. 7d) shows two peaks, respectively at 53 and 148 °C. These two temperatures are close to those obtained during 4% Rh/CeO_2 (DP) reduction. The small differences which exist could be due to the fact that in the latter, Rh_2O_3 is formed upon calcination of $RhCl_3$. The reduction peak at 60 °C was attributed to the reduction of Rh_2O_3 and O_2^- ions present on the CeO_2 surface whereas the peak at 141 °C could be due to the reduction of Rh_2O_3 and O_2^- ions rather located in the bulk (not on the surface) [36]. It was stated that the existence of two reduction peaks is due to the reduction of Rh_2O_3 in different environments and/or with different particle size [13, 37]. Rh_2O_3 is reduced into Rh^0 [35, 38-39]. Conversely, Boutros et al. [37] stated that the first reduction peak (at lower temperature) is due to the reduction of Rh_2O_3 into Rh_2O and RhO and the second one to the reduction of Rh_2O and RhO.

The TPR profile of 4% Rh/CeO_2 (Imp) shows an intense peak at 82 °C and a small peak at 204 °C. The first peak could be ascribed to the reduction of the Rh^{4+} clusters –evidenced by EPR– into Rh^{3+} and Rh^{2+}. Indeed, EPR showed the reduction of Rh^{4+} clusters after one hour under vacuum at 400 °C. The peak at 204 °C could be due to the reduction of some Rh^{3+} ions, located in the bulk, into Rh^{2+}.

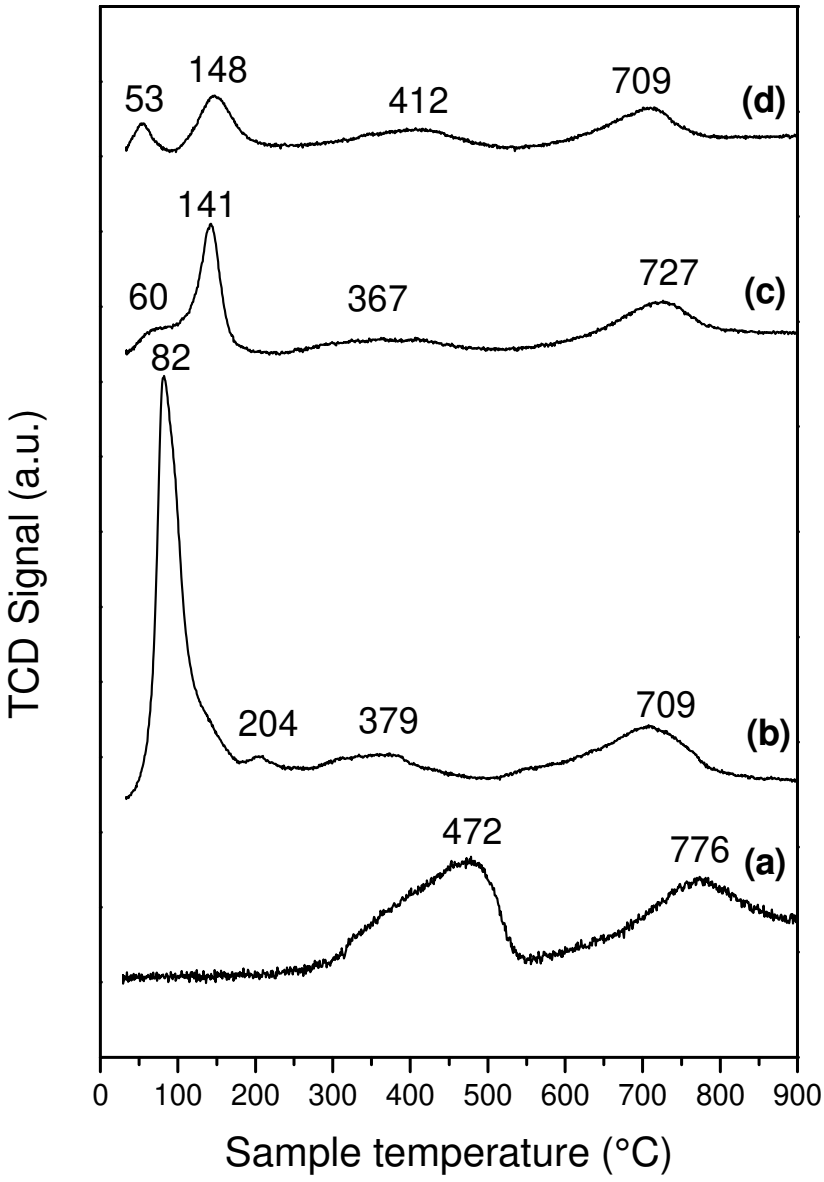

Figure 7: TPR profiles: a) CeO_2, b) 4% Rh/CeO_2 (Imp), c) 4% Rh/CeO_2 (DP), d) 4% Rh_2O_3/CeO_2 (DP).

3.2. Catalytic tests

3.2.1. Oxidation of propylene

Fig. 8 illustrates the conversion of propylene versus the reaction temperature in the presence of the pure ceria support and the 4% Rh/CeO_2 catalysts. The catalyst 0.5 % Rh/CeO_2 (Imp) was also evaluated. It is observed that addition of rhodium shifts the temperature of propylene conversion to lower values, whatever is the rhodium content or the preparation method. Furthermore, it is worthy to note that in all cases, propylene was exclusively converted into CO_2. No other by-product was formed.

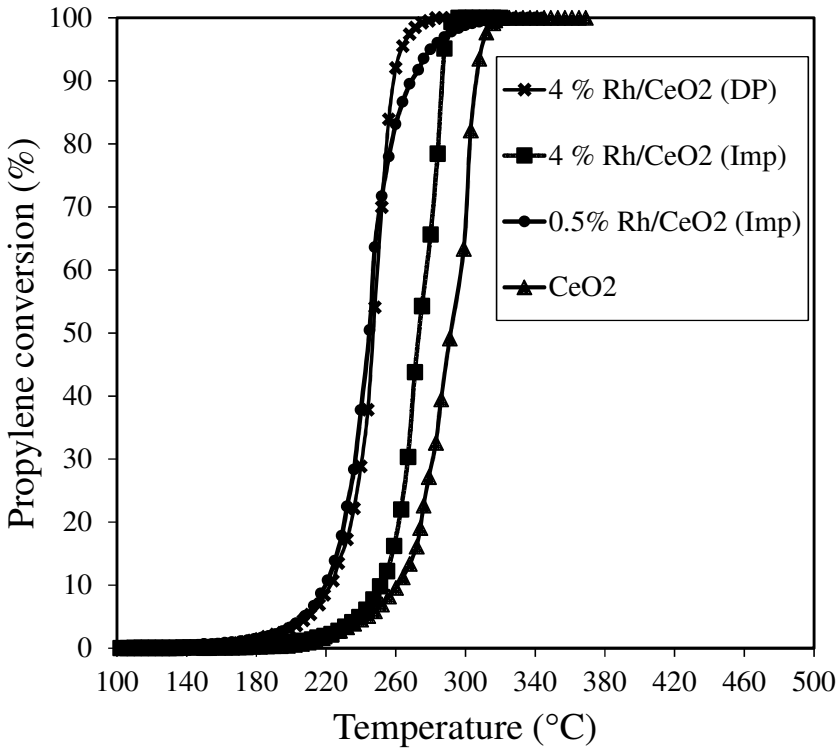

Figure 8: Conversion of propylene during its total oxidation versus reaction temperature over CeO_2, 4 % Rh/CeO_2 (DP), 4 % Rh/CeO_2 (Imp), and 0.5 % Rh/CeO_2 (Imp).

Furthermore, 4 % Rh/CeO_2 (DP) is more reactive than 4 % Rh/CeO_2 (Imp), with a ($T_{50(Imp)}$ - $T_{50(DP)}$) of about 35 °C, T_{50} being the temperature of 50 % propylene conversion. This result is in agreement with those reported in the literature [3, 16, 33-34] where the deposition–

precipitation method gave better activities in oxidation reactions than the impregnation one. Indeed, the deposition-precipitation leads to the formation of nanosized particles dispersed on the surface of the solid, which are highly efficient in catalysis, whereas the impregnation method leads to the formation of large particles. The size of these particles depends in general on the active sites concentration added on the support. It decreases with this latter parameter and can become the same dimensions as those of nanoparticles. Indeed, it was demonstrated that when catalysts are prepared by the impregnation method with low rhodium contents, 0.5% Rh/CeO_2 (Imp), its catalytic activity is similar to that obtained for the 4% Rh/CeO_2 (DP).

Other factors could be also in the origin of the higher performance of the 4% Rh/CeO_2 (DP). This catalyst exhibits also the presence of O_2^- species along with the presence of Rh_2O_3 phase and also lower reduction temperatures in TPR than 4% Rh/CeO_2 (Imp). All these factors could favor higher activities in oxidation reactions.

3.2.2. Combustion of carbon black

Fig. 9 shows the three temperatures, T_i, T_{max}, and T_f, obtained for the different catalysts during the total oxidation of the carbon black. T_{max} was used to compare the catalytic activity. The performance of 4% Rh/CeO_2 (DP) is better than that of CeO_2 particularly in T_i and T_f and much better than 4% Rh/CeO_2 (Imp) with a noticeable difference in temperatures. The better performance of the DP-solid could be due, as in the case of propylene, to the presence of Rh_2O_3 and O_2^- as well as to the better reducibility and lower particle size on the solid surface. Indeed, when the size of large particles decreases by decreasing the rhodium content in the Imp solid (0.5% Rh/CeO_2 (Imp)), the combustion activity increases and became similar to that obtained for the DP-solid.

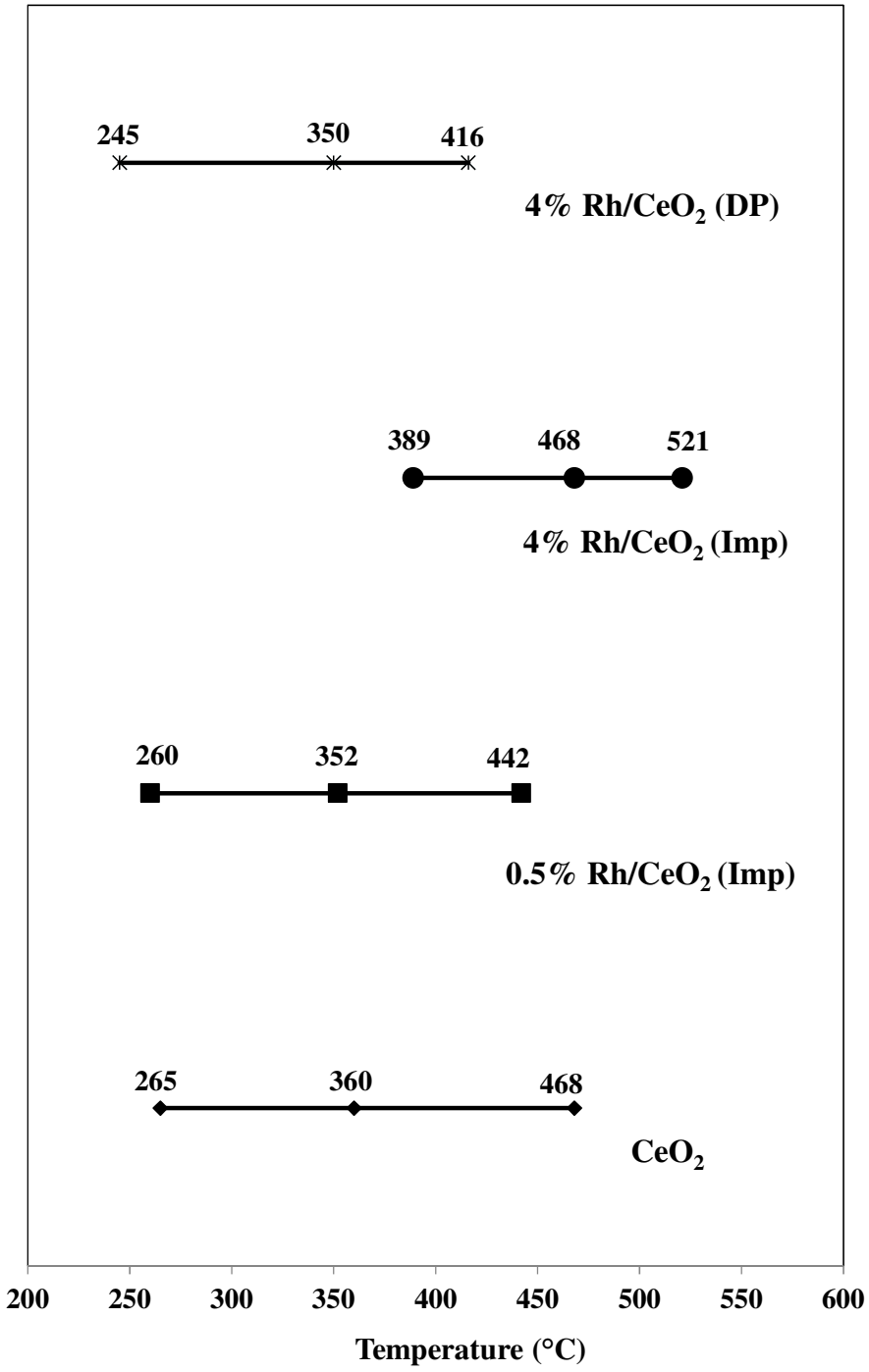

Figure 9: The temperatures (T_i, T_{max}, and T_f) of total carbon black oxidation over the catalysts CeO_2, 4 % Rh/CeO_2 (DP), 4 % Rh/CeO_2 (Imp), and 0.5 % Rh/CeO_2 (Imp).

Conclusion

The impregnation (Imp) and the deposition-precipitation (DP) methods were used to introduce 4 wt % of Rh, using $RhCl_3$ as precursor, on CeO_2. A calcination at 400 °C for 4 h followed this step. DP method results in the formation of weakly attached O_2^- species on ceria surface, identified by EPR, and in the formation of the oxide Rh_2O_3. Both species were not obtained by Imp method. These species are responsible for the better catalytic performance of 4%Rh/CeO_2 (DP) solid in the total oxidation of propylene and carbon black reactions. The easier reducibility of rhodium oxides species and the lower size of rhodium particles are also in the origin of the higher catalytic activities of the solids prepared by DP method.

Acknowledgments

The University of Littoral – Côte D'Opale (ULCO), the Lebanese University, and the Agence Universitaire de la Francophonie – Région du Moyen-Orient (AUF) are gratefully acknowledged for financial supports. The authors would also like to thank the ARCUS E2D2 project, the French Ministry of Foreign Affairs, and the «Région Hauts de France» for financial support.

Conflict of interest

There is no conflict of interest to disclose.

References

[1] Z. Qu, F. Yu, X. Zhang, Y. Wang, J. Gao, Support effects on the structure and catalytic activity of mesoporous Ag/CeO_2 catalysts for CO oxidation, Chem. Eng. J. 229 (2013) 522-532.
https://doi.org/10.1016/j.cej.2013.06.061

[2] C. Guimarães Maclel, T. de Freitas Silva, M. Iuki Hirooka, M.N. Belgacem, J.M. Assaf, Effect of nature of ceria support in CuO/CeO_2 catalyst for PROX-CO reaction, Fuel 97 (2012) 245-252.
https://doi.org/10.1016/j.fuel.2012.02.004
[3] M. Skaf, S. Aouad, S. Hany, R. Cousin, E. Abi-Aad, A. Aboukaïs, Physicochemical characterization and catalytic performance of 10 % Ag/CeO_2 catalysts prepared by impregnation and deposition–precipitation, J. Catal. 320 (2014) 137-146.
https://doi.org/10.1016/j.jcat.2014.10.006
[4] I. Luz, F.X. Llabrés Xamena, A. Corma, Bridging homogeneous and heterogeneous catalysis with MOFs: « Click » reactions with Cu-MOF catalysts, J. Catal. 276 (2010) 134-140.
https://doi.org/10.1016/j.jcat.2010.09.010
[5] S. Hany, M. Skaf, S. Aouad, C. Gennequin, M. Labaki, E. Abi-Aad, A. Aboukaïs, Correlation between the size and the magnetic properties of Ag^{2+} clusters loaded on ceria surface and their catalytic performance in the total oxidation of propylene. EPR study, Chem. Phys. 502 (2018) 1-5.
https://doi.org/10.1016/j.chemphys.2018.01.001
[6] M. Haneda, T. Kaneko, N. Kamiuchi, M. Ozawa, Improved three-way catalytic activity of bimetallic Ir-Rh catalysts supported on CeO_2-ZrO_2, Catal. Sci. Technol. 5(3) (2015) 1792-1800.
https://doi.org/10.1039/c4cy01502a
[7] T. Shimizu, M. Ota, Y. Sato, H. Inomata, Y. Nakagawa, T. Nanba, Preparation of Rh/CeO_2 using supercritical CO_2 and its catalytic application for automotive exhaust, J. Jpn Petrol. Inst. 56(5) (2013) 312-316.
https://doi.org/10.1627/jpi.56.312
[8] X. Li, F. Wang, X. Pan, X. Bao, Rh/CeO_2-SiC as a catalyst in partial oxidation of ethanol for hydrogen production, Chinese J. Catal. 34(1) (2013) 257-262.
https://doi.org/10.3724/SP.J.1088.2013.30105
[9] I. Cuauhtémoc, G. Del Angel, G. Torres, V. Bertin, Catalytic wet air oxidation of gasoline oxygenates using Rh/γ-Al_2O_3 and Rh/γ-Al_2O_3-CeO_2 catalysts, Catal. Today 133-135 (1-4) (2008) 588-593.
https://doi.org/10.1016/j.cattod.2008.02.006
[10] C. Force, J. P. Belzunegui, J. Sanz, A. Martínez-Arias, J. Soria, Influence of precursor salt on metal particle formation in Rh/CeO_2 catalysts, J. Catal. 197 (2001) 192-199.

https://doi.org/10.1006/jcat.2000.3067
[11] D.I. Kondarides, Z. Zhang, X.E. Verykios, Chlorine-induced alterations in oxidation state and CO chemisorptive properties of CeO_2-supported Rh catalysts, J. Catal. 176 (1998) 536-544.
https://doi.org/10.1006/jcat.1998.2064
[12] A. Martínez-Arias, J. Soria, J.C. Conesa, Spectroscopic study of active phase-support interactions on a RhO_x/CeO_2 catalyst: Evidence for electronic interactions, J. Catal. 168 (1997) 364-373.
https://doi.org/10.1006/jcat.1997.1684
[13] R.S. Mulukutla, T. Shido, K. Asakura, T. Kogure, Y. Iwasawa, Characterization of rhodium oxide nanoparticles in MCM-41 and their catalytic performances for NO-CO reactions in excess O_2, Appl. Catal. A 228 (2002) 305-314.
https://doi.org/10.1016/S0926-860X(01)00992-9
[14] E. Abi-Aad, J. Matta, R. Flouty, C. Decarne, S. Siffert, A. Aboukaïs, EPR investigation at 4 K of ceria and Cu-Ce oxide under SO_2 and H_2 atmosphere, Magn. Res. Coll. Interf. Sci. 76 (2002) 479-484.
https://doi.org/10.1007/978-94-010-0534-0_42
[15] Y. Liu, C. Wen, Y. Guo, G. Lu, Y. Wang, Effects of surface area and oxygen vacancies on ceria in CO oxidation: differences and relationships, J. Mol. Catal. A 316 (2010) 59-64.
https://doi.org/10.1016/j.molcata.2009.09.022
[16] A. Aboukaïs, S. Aouad, M. Skaf, S. Hany, M. Labaki, R. Cousin, E. Abi-Aad, EPR investigation of the nature of oxygen species present on the surface of gold impregnated cerium oxide, Mater. Chem. Phys. 170 (2016) 285-293.
https://doi.org/10.1016/j.matchemphys.2015.12.053
[17] A. Aboukaïs, E.A. Zhilinskaya, J.-F. Lamonier, I.N. Filimonov, EPR study of ceria–silica and ceria–alumina catalysts: Localization of superoxide radical anions, Colloids Surf. A 260 (2005) 199-207.
https://doi.org/10.1016/j.colsurfa.2005.02.036
[18] A.V. Kucherov, S.G. Lakeev, M. Shelef, ESR study of Rh/γ-Al_2O_3 and Rh/HZSM-5 promoted by Cu^{2+}, Gd^{3+}, and PO_4^{3-}, Appl. Catal. B 16 (3) (1998) 245-254.
https://doi.org/10.1016/S0926-3373(97)00080-5.
[19] E. Abi-Aad, R. Bechara, J. Grimblot, A. Aboukaïs, Preparation and characterization of ceria under an oxidizing atmosphere. Thermal analysis, XPS, and EPR study, Chem. Mater. 5 (1993) 793-797.

https://doi.org/10.1021/cm00030a013
[20] J.L.G. Fierro, J. Soria, J. Sanz, M.J. Rojo, Induced changes in ceria by thermal treatments under vacuum or hydrogen, J. Solid State Chem. 66 (1987) 154-162.
https://doi.org/10.1016/0022-4596(87)90230-1
[21] K. W. Blazey, F. Levy, EPR of rhodium, osmium and iridium-doped rutile, Solid State Commun. 59 (6) (1986) 335-338.
https://doi.org/10.1016/0038-1098(86)90558-2
[22] S.B. Sinha, D.Y. Shopov, L.S. Sharninghausen, D.J. Vinyard, B.Q. Mercado, G.W. Brudvig, R.H. Crabtree, A Stable Coordination Complex of Rh(IV) in an N,O-Donor Environment, J. Am. Chem. Soc. 137 (2015) 15692-15695.
https://doi.org/10.1021/jacs.5b12148
[23] J. Soria, J.C. Conesa, A. Martínez-Arias, Characterization of surface defects in CeO_2 modified by incorporation of precious metals from chloride salts precursors: an EPR study using oxygen as probe molecule, Colloids Surf. A 158 (1999) 67-74.
https://doi.org/10.1016/S0927-7757(99)00132-6
[24] R. Flouty, E. Abi-Aad, S. Siffert, A. Aboukaïs, Influence of molybdenum on ceria activity and CO_2 selectivity in propene total oxidation, Kinet. Catal. 45 (2) (2004) 219-226.
https://doi.org/10.1023/B:KICA.0000023795.58615.b2
[25] X-X. Zhang, B. B. Wayland, Sterically Demanding Diporphyrin Ligands and Rhodium (II) Porphyrin Bimetalloradical Complexes, Inorg. Chem. 39 (2000) 5318-5325.
https://doi.org/10.1021/ic0006302
[26] A. Varela-Álvarez, T. Yang, H. Jennings, K.P. Kornecki, S.N. Macmillan, K.M. Lancaster, J.B. C. Mack, J. Du Bois, J.F. Berry, D.G. Musaev, Rh2(II,III) Catalysts with chelating carboxylate and carboxamidate supports: electronic structure and nitrene transfer reactivity, J. Am. Chem. Soc. 138 (2016) 2327-2341.
https://doi.org/10.1021/jacs.5b12790
[27] H. Gustafsson, M. Danilczuk, M.D. Sastry, A. Lund, E. Lund, Enhanced sensitivity of lithium dithionates doped with rhodium and nickel for EPR dosimetry, Spectrochim. Acta A 62 (2005) 614-620.
https://doi.org/10.1016/j.saa.2005.01.024
[28] C-C. Ding, S-Y. Wu, L-J. Zhang, G-L. Li, Z-H. Zhang, Theoretical investigations on the defect structures and spin Hamiltonian parameters for various orthorhombic Rh^{2+} centres in $KTiOPO_4$ and $KTiOAsO_4$, Physica B 479 (2015) 21-25.
https://doi.org/10.1016/j.physb.2015.09.026

[29] M. Tanabe, H. Matsuoka, Y. Ohba, S. Yamauchi, K. Sugisaki, K. Toyota, K. Sato, T. Takui, I. Goldberg, I. Saltsman, Z. Gross, Time-Resolved Electron Paramagnetic Resonance and Phosphorescence Studies of the Lowest Excited Triplet States of Rh(III) Corrole Complexes, J. Phys. Chem. A 116 (2012) 9662-9673.
https://doi.org/10.1021/jp3071037
[30] L. Kępiński, J. Okal, Occurrence and Mechanism of Formation of CeOCl in Pd/CeO_2 Catalysts, J. Catal. 192 (2000) 48-53.
https://doi.org/10.1006/jcat.200.2823
[31] E. Moran Miguelez, M. A. Alario Franco, J. Soria, An EPR study of rhodium oxihydroxide. J. Solid State Chem. 46 (1983) 156-161.
https://doi.org/10.1006/0022-4596(83)90136-6
[32] H.-M. Zhang, S.-Y. Wu, P. Xu, L.-L. Li, Theoretical studies of the local structures and EPR parameters for various Rh^{2+} centers in AgCl, J. Mol. Struc. - Theochem 953 (2010) 157-162.
https://doi.org/10.1016/j.theochem.2010.05.021
[33] A. Aboukaïs, M. Skaf, S. Hany, R. Cousin, S. Aouad, M. Labaki, E. Abi-Aad, A comparative study of Cu, Ag and Au doped CeO_2 in the total oxidation of volatile organic compounds (VOCs), Mater. Chem. Phys. 177 (2016) 570-576.
https://doi.org/10.1016/j.matchemphys.2016.04.072
[34] M.I. Zaki, G.A.M. Hussein, S.A.A. Mansour, H.M. Ismail, G.A.H. Mekhemer, Ceria on silica and alumina catalysts: dispersion and surface acid-base properties as probed by X-ray diffractometry, UV-Vis diffuse reflectance and in situ IR absorption studies, Colloids Surf. A 127 (1997) 47-56.
https://doi.org/10.1016/S0927-7757(96)03943-X
[35] A. Bueno-López, I. Such-Basáñez, C. Salinas-Martínez de Lecea, Stabilization of active Rh_2O_3 species for catalytic decomposition of N_2O on La-, Pr-doped CeO_2, J. Catal. 244 (2006) 102-112.
https://doi.org/10.1016/j.jcat.2006.08.021
[36] M. Ozawa, M. Takahashi-Morita, K. Kobayashi, M. Haneda, Core-shell type ceria zirconia support for platinum and rhodium three way catalysts, Catal. Today 281 (2017) 482-489.
https://doi.org/10.1016/j.cattod.2016.06.029

[37] M. Boutros, F. Launay, A. Nowicki, T. Onfroy, V. Herledan-Semmer, A. Roucoux, A. Gédéon, Reduced forms of Rh(III) containing MCM-41 silicas as hydrogenation catalysts for arene derivatives, J. Mol. Catal. A 259 (2006) 91-98.
https://doi.org/10.1016/j.molcata.2006.06.007
[38] J. C. Vis, H. F. J. van't Blik, T. Huizinga, J. van Grondelle, R. Prins, The morphology of rhodium supported on TiO_2 and Al_2O_3 as studied by temperature-programmed reduction-oxidation and transmission electron microscopy, J. Catal. 95 (1985) 333-345.
https://doi.org/10.1016/0021-9517(85)90111-3
[39] H. Liu, Z. Ma, Rh_2O_3/monoclinic $CePO_4$ composite catalysts for N_2O decomposition and CO oxidation, Chinese J. Chem. Eng. 26 (2018) 109-115.
https://doi.org/10.1016/j.cjche.2017.02.007